Finite Element Analysis of Skin Effect Resistance in Submillimeter Wave Schottky Barrier Diodes

JOHN S. CAMPBELL AND GERARD T. WRIXON, MEMBER, IEEE

Abstract—**The skin effect resistance of GaAs Schottky barrier diodes, operating at high frequency, has been obtained using a specially developed finite element computer program. The devices were analyzed as multiplane finite element models entailing curved high-order numerically integrated isoparametric elements. These models coped easily with complexity of shape and with the near singularity associated with the geometry of the anode. A parametric study entailing twenty-six analyses was carried out, from which it was concluded that the skin effect resistance can be minimized by the correct choice of topographical features such as the extent of the ohmic contact and the anode shape.**

I. INTRODUCTION

IN RECENT YEARS the submillimeter and far infrared wavelength bands have seen the emergence of low noise superheterodyne mixing techniques that hitherto had been confined to microwave and millimeter wavelengths. Workers in the fields of radio astronomy, plasma diagnostics, and spectroscopy have been among the first to benefit from these techniques which have placed the benefits of coherent detection and, in particular, the availability of broad-band multichannel spectrometers, at their disposal for the first time.

The GaAs Schottky barrier diode is the universally used nonlinear mixing element in high frequency receivers [1]. It is a wide bandwidth device having high sensitivity and good mechanical stability. It can be operated satisfactorily at room temperature but its sensitivity can increase by a factor of up to seven when cooled to cryogenic temperatures. It consists of a small metal contact deposited on an epitaxial GaAs layer on a heavily doped substrate, the junction being mechanically contacted when mounted in a mixer circuit.

The conversion loss L of a mixer is the ratio of the power from the RF source to the power absorbed in the IF load. A considerable fraction of this conversion loss occurs in the diode arising from two separate processes, the intrinsic conversion loss L_0 and the parasitic conversion loss L_p. L_0 is the result of losses arising from the conversion process within the nonlinear resistance of the diode and for a broadband mixer has a theoretical minimum of 3 dB. L_p is the loss associated with the parasitic elements of the diode, namely, the junction capacitance C_0 and the series resistance R_s.

It has been shown [2] that the series resistance R_s of a Schottky barrier diode is strongly frequency-dependent due to skin effect and carrier plasma resonance. While it is possible to minimize the effect of the latter by choosing carrier concentrations whose plasma resonance lies well outside the diode operating range, skin effect resistance is a monotonically increasing function of frequency and for diodes in the submillimeter range it can form a major proportion of the total series resistance [1].

The aim of this investigation is to determine whether the skin effect resistance R_{sk} can be minimized by the correct choice of diode topography, in particular, the shape of the anode and the position of the ohmic contact. The availability of E-beam lithography has meant that submicron noncircular anode shapes can be employed if these should prove to be beneficial. In fact, earlier theoretical and experimental investigations [3], [4] have shown that it is possible to reduce the dc spreading resistance by increasing the perimeter to area ratio of the anode while maintaining a constant area of diode and, hence, also a constant capacitance. Wrixon and Pease [3] fabricated cross-shaped epitaxial diodes with anode area equal to that of 1-μm-diameter circular diode and confirmed that the spreading resistance was reduced by 30 percent while the capacitance remained unchanged.

The analysis of semiconductor devices is not possible for practical devices unless recourse is made to computer based numerical simulation techniques. The development of such techniques for semiconductor devices started with the use of a one-dimensional finite difference model [5], and this approach was later extended to the two-dimensional case [6]. More recently, simulation of two-dimensional effects have been made [7], [8] using the finite element method, which more readily accommodates geometric irregularities and facilitates mesh grading. In this present paper, a multiplane finite element model, using curved high-order

Manuscript received August 19, 1981; revised December 28, 1981.

J. S. Campbell is with the Department of Civil Engineering, University College, Cork, Ireland

G. T. Wrixon is with the Microelectronics Research Center, University College, Cork, Ireland.

0018-9480/82/0500-0744$00.75 ©1982 IEEE

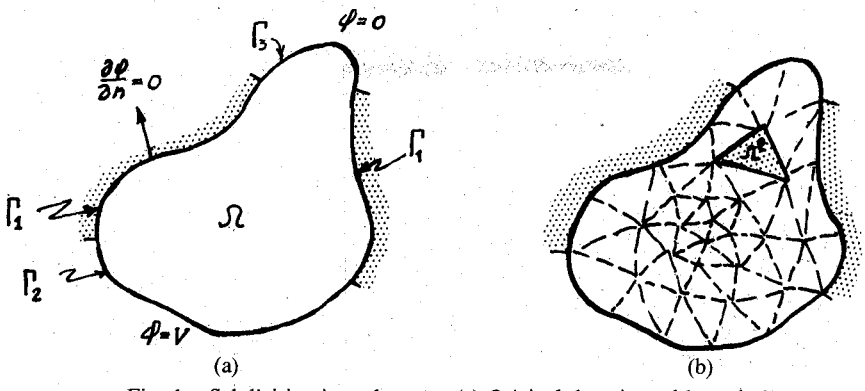

Fig. 1. Subdivision into elements. (a) Original domain and boundaries. (b) Finite element subdivision.

elements, is developed for the analysis of Schottky barrier diodes operating at high frequency.

II. Governing Equations and Variational Approach

For Schottky barrier diodes, Langley [4] has shown that, outside of the space change region, the general time dependent equations reduce to the simple Laplace type equation of electrostatics. Thus at any point x, inside domain Ω (Fig. 1), the solution must satisfy the divergence condition

$$\nabla\cdot\sigma\nabla\phi=0. \tag{1}$$

On the boundaries, the solution ϕ must satisfy the conditions

$$\frac{\partial\phi}{\partial n}=0, \quad \text{on part } \Gamma_1 \text{ (Neuman condition)} \tag{2}$$

$$\phi-V=0, \quad \text{on part } \Gamma_2 \text{ (Dirichlet condition)}$$

$$\phi=0, \quad \text{on part } \Gamma_3 \text{ (Dirichlet condition)} \tag{3}$$

where ϕ is the scalar potential function, σ is the conductivity, n is the normal direction to the boundary, V is a prescribed potential, and $\Gamma_1+\Gamma_2+\Gamma_3=\Gamma$, the total boundary (Fig. 1).

In the variational approach [9], the direct solution of the governing partial differential equation (pde) and the boundary conditions (bc) are supplanted by the minimization of a functional which has the governing pde+bc as its Euler–Lagrange equations. The differential and variational approaches are equivalent: a solution satisfying the pde+bc minimizes the functional; minimization of the functional gives a solution which satisfies the pde+bc. It is easily shown that, for this electrostatics problem, the required functional is given by

$$\Pi(\phi)=\frac{1}{2}\int_\Omega\sigma(\nabla\phi)^2\,d\Omega. \tag{4}$$

Applying Green's theorem to this functional gives

$$\Pi(\phi)=\tfrac{1}{2}\int_\Gamma\phi\sigma\nabla\phi\cdot n\,d\Gamma-\int_\Omega\phi\nabla\cdot(\sigma\nabla\phi)\,d\Omega \tag{5}$$

in which the volume integral is identically zero (from (1)), the boundary integral is zero on the ohmic contact ($\phi=0$), and also on nonconducting boundaries ($\nabla\phi\cdot n=0$). For the diodes considered here, the boundary integral is nonzero only on the anode Γ_2, where the potential $\phi=V$ is constant and therefore (5) reduces to

$$\Pi(\phi)=\frac{V}{2}\int_{\Gamma_2}\sigma\nabla\phi\cdot n\,d\Gamma=\frac{V}{2}I \tag{6}$$

in which I is the total current passing from the anode to the ohmic contact. From (4) and (6) it follows that the total current I may be written as

$$I=\int_\Omega\sigma(\nabla\phi)^2\,d\Omega/V$$

and hence the skin effect resistance, defined as $R_{sk}=V/I$, is given by

$$R_{sk}=V^2\Big/\int_\Omega\sigma(\nabla\phi)^2\,d\Omega. \tag{7}$$

III. Finite Element Approach

The finite element method is a numerical technique which enables an approximate solution to be obtained for boundary value problems. The essence of the finite element method consists of two steps.

i) The total domain Ω is subdivided into a number of smaller contiguous subdomains Ω^e (the elements) as shown in Fig. 1(b).

ii) The dependent variable ϕ is defined in a piecewise continuous manner, across the complete domain, in terms of a finite numbered set of discrete nodal parameters. Within each element, the piecewise description on the dependent variable ϕ is given as

$$\phi(x)=N_i(x)u_i \tag{8}$$

in which repeated subscripts imply summation. Here $N_i(x)$ are prescribed polynomial functions and u_i are the values of ϕ at the discrete locations x_i, known as the nodal points. These nodal points are usually located on the external

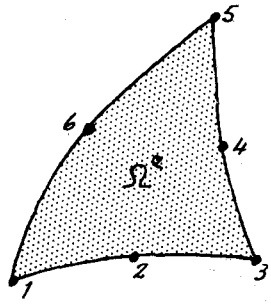

Fig. 2. Six-noded curved triangular element used in the diode analysis.

boundary of the element. To be specific; in the diode analysis a triangular element with curved edges is used, having 3 vertex and 3 midside nodes as shown in Fig. 2.

Equation (8) describes an approximation to the *continuous* function $\phi(x)$ in terms of a *discrete* number of nodal variables u_i. It follows from (8) that the gradient is given by

$$\nabla\phi = \nabla N_i u_i \tag{9}$$

and therefore the functional of (4) may be rewritten as

$$\Pi(\phi) = \sum_e \Pi^e$$

$$= \sum_e \int_{\Omega^e} \tfrac{1}{2}\sigma(\nabla N_i u_i)(\nabla N_j u_j)\, d\Omega \tag{10}$$

where the summation is taken over all the elements e. The minimization referred to in Section II is now carried out with respect to the *discrete* variables u_i. Thus, for a minimum, the condition $\partial\Pi/\partial u_i = 0$ is applied, leading to

$$K_{ij}u_j = 0 \tag{11}$$

in which

$$K_{ij} = \sum_e k_{ij}^e$$

and

$$k_{ij}^e = \int_{\Omega^e} \sigma \nabla N_i \nabla N_j d\Omega \tag{12}$$

is the element matrix.

Applying the Dirichlet boundary conditions to each of the nodes on boundary Γ_2 then (11) becomes

$$K_{ij}^* u_j = p_i. \tag{13}$$

These equations may be solved (using, for example, Gaussian Elimination) to obtain the nodal potentials u_j. A particular feature of the formulation is that these linear simultaneous equations are symmetric, positive definite, and strongly banded. The frontal equation solution procedure [10] used here exploits these enhancing properties. The solution set $\{u_j\}$ describes the variation of the scalar potential $\phi(x)$ in a discrete, pointwise form. Using this solution subsidiary computations may easily be made to obtain other physical parameters at all points within the domain.

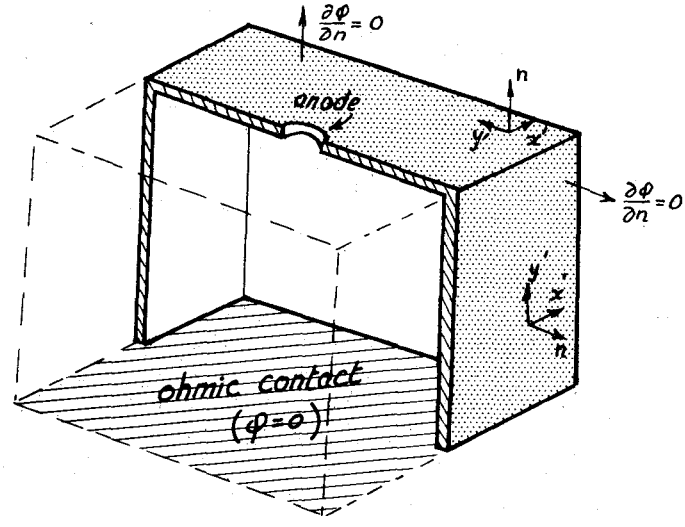

Fig. 3. Cut away view of skin-effect multiplane model.

IV. Multiplane Finite Element Model

For diodes operating at high frequency, the current flow is constricted within a skin region at the outside surface of the diode. For the diodes considered here the current flow takes place in the multiplane, hollow box shaped region shown in Fig. 3. For each plane, it may be reasonably assumed that the potential does not vary through the skin depth δ. Thus the $x-y$ planes in Fig. 3 may be analyzed using plane, two-dimensional finite elements of thickness δ. At the 'folds', where the top and sides meet, a common nodal potential u_k is shared by each adjacent plane, thus ensuring continuity of the potential ϕ. For the multiplane models the integral of (12) becomes

$$k_{ij} = \int_{\Omega^e} \sigma \nabla N_i \nabla N_j \delta\, dx'dy'$$

where $x'y'$ are the in-plane local coordinates as shown in Fig. 3.

A six-noded triangular element having curved edges, shown in Fig. 2, was used because this greatly simplifies the task of mesh grading. The six-noded quadratic high-order numerically integrated element was chosen in

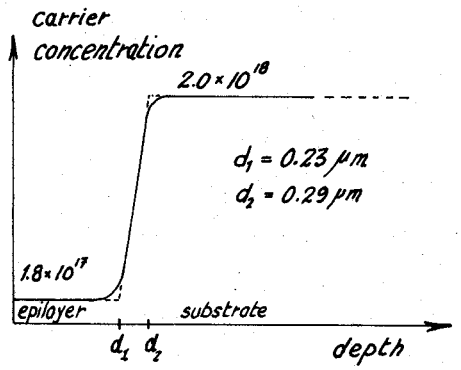

Fig. 4. Carrier concentration profile for GaAs diode.

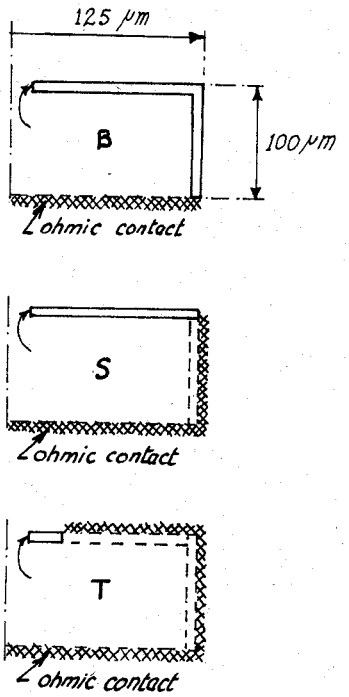

Fig. 5. Ohmic contact configurations for high frequency model illustrated on diode cross section. Key: *B*: bottom; *S*: side, *T*: top.

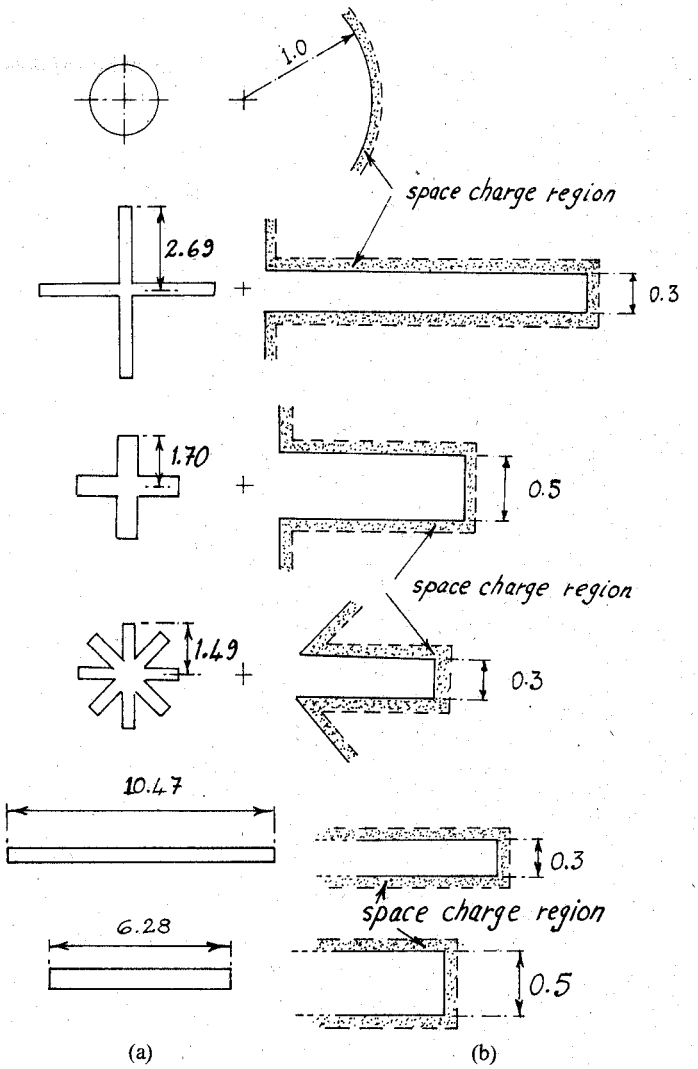

Fig. 6. Anode shapes for high frequency analyses for anodes having cross-sectional area of $\pi(\mu m)^2$. (a) Shape of etched anode. (b) Magnified view showing the space charge region. (All dimensions in μm.)

preference to the simple three-noded linear triangular element for two main reasons: firstly, curved boundaries are more easily and more accurately dealt with; and secondly, considerably less data is required for mesh definition. Zienkiewicz [11] gives full details of the curvilinear coordinates, element functions, numerical integration, etc., employed in computing the matrices for these elements.

V. Optimization of Diode Topography

The optimal diode topography was determined via a parametric study. The skin effect resistance R_{sk} was computed for twenty-six physically realizable diode configurations in which the anode geometry and the ohmic contact region were varied.

The carrier concentration profile for the GaAs epitaxial layer is given in Fig. 4, and the width of the space charge region was computed at $t = 780$ Å using the formula

$$t = \sqrt{\frac{2\epsilon_s \phi_i}{qN_d}}$$

in which ϵ_s is the permittivity of the GaAs, q is the electronic charge, ϕ_i is the built-in barrier voltage, and $N_d = 1.8 \times 10^{17}$ is the doping density. The skin depth δ was computed as $\delta = 2.37$ μm using the formula

$$\delta = (\mu \Pi f \sigma)^{-1/2}$$

in which μ is the permeability of GaAs, $f = 400$ GHz is the frequency, and σ is the conductivity of the epilayer.

Three ohmic contact configurations, shown in Fig. 5, were considered and two different anode areas of $\Pi/4(\mu m)^2$ and $\Pi(\mu m)^2$ were used for the etched anode areas. The space charge region, of width 780 Å, surrounding the anode, increased the effective anode area as shown in Fig. 6. Circular, cruciform, octoform (8-arm), and rect-

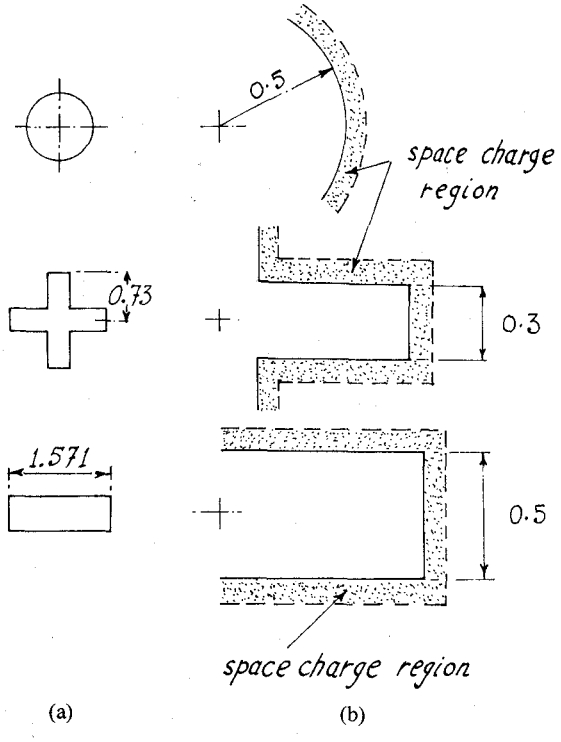

Fig. 7. Anode shapes for high frequency analyses for anodes having cross-sectional area of $\pi/4(\mu m)^2$. (a) Shape of etched anode. (b) Magnified view showing space charge region. (All dimensions in μm).

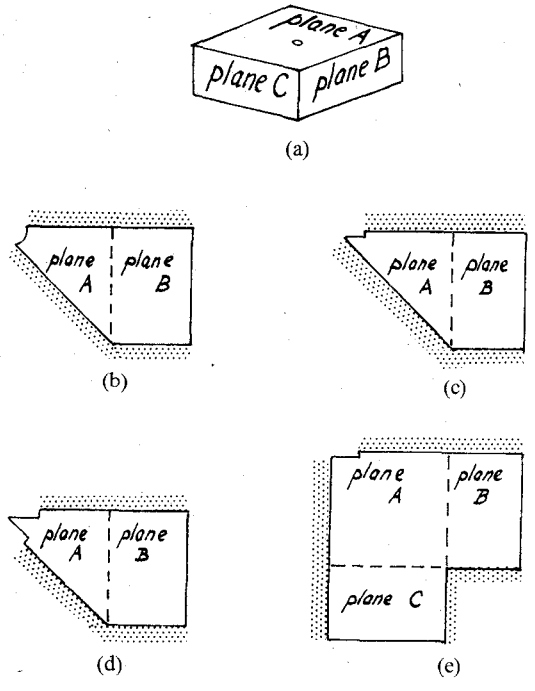

Fig. 8. Use of symmetry to reduce the extent of the region analyzed. (Axes of symmetry shown shaded.) (a) Multiplane hollow box model. (b) Circular anode. (c) Cruciform anode. (d) 'Octoform' anode. (e) Rectangular slot anode.

angular shaped anode geometries were included as shown in Figs. 6 and 7. By utilizing multiple symmetries, as shown in Fig. 8, the finite element mesh region was reduced by

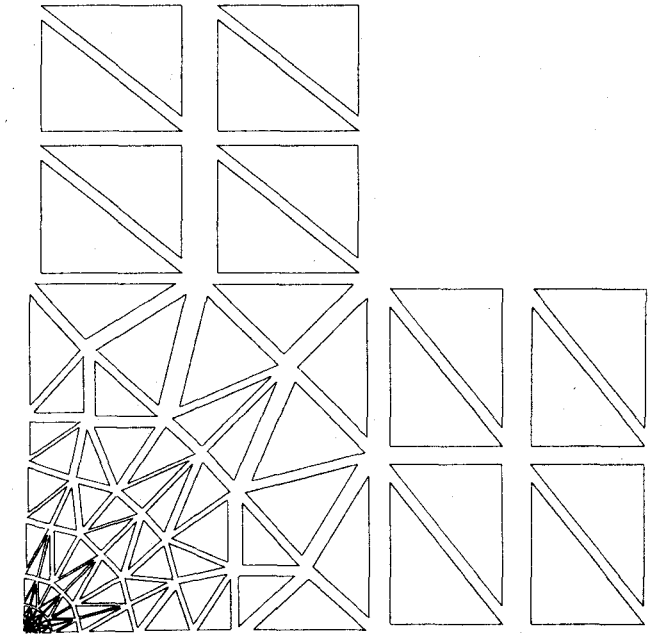

Fig. 9. Developed plot of finite element mesh in which each element is shown shrunk about its centroid. Due to symmetry only one quadrant of the diode is considered in the analysis. (Magnification of the anode region is shown in Fig. 10.)

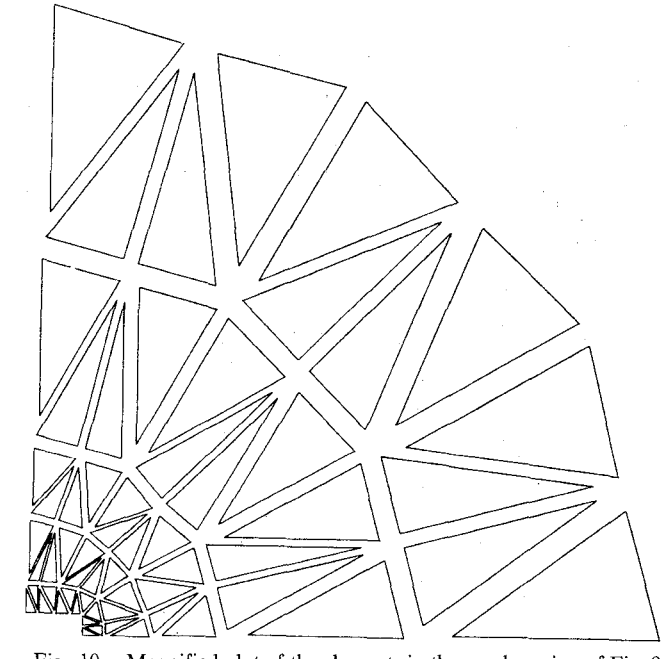

Fig. 10. Magnified plot of the elements in the anode region of Fig. 9.

factors of 4 or 8. A typical mesh, for a rectangular anode, is shown in Figs. 9 and 10. The extreme concentration of elements in the anode region and the ease of mesh grading using the 6-noded triangular elements should be noted in these figures.

The skin effect resistance R_{sk} for each of the twenty-six configurations is given in Tables I and II. Additional information, computed in each analysis, but not detailed

TABLE I
COMPUTED SKIN RESISTANCE R_{sk} AT 400 GHz FOR ANODES HAVING AREA OF $\pi(\mu m)^2$

Analysis Label	Anode Shape	Ohmic Contact Configuration	Skin Effect Resistance R_{SK}
AI.I	 2 μm	B	4.445
AI.2		S	3.905
AI.3		T	2.0II
A3.I	 0.3 μm	B	3.864
A3.2		S	3.324
A3.3		T	I.43I
A4.I	 0.5 μm	B	4.I53
A4.2		S	3.6I3
A4.3		T	I.7I9
A7.I	 0.3 μm	B	4.I64
A7.2		S	3.624
A7.3		T	I.730
AII.I	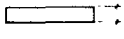 0.5 μm	B	3.97I
AII.2		S	3.432
AII.3		T	I.608
AI2.I	0.3 μm	B	3.640
AI2.2		S	3.098
AI2.3		T	1.272

Key: *B* is the ohmic contact on back of chip only; *S* is the ohmic contact on back and side of chip; *T* is the ohmic contact on back, side, and top to within 13 μm of the anode.

TABLE II
COMPUTED SKIN RESISTANCE R_{sk} AT 400 GHz FOR ANODES HAVING AREA OF $\pi/4(\mu m)^2$

Analysis Label	Anode Shape	Ohmic Contact Configuration	Skin Effect Resistance R_{SK}
A2.I	 1 μm	B	4.94I
A2.2		S	4.40I
A2.3		T	2.508
A5.I	 0.3 μm	B	4.746
A5.2		S	4.206
A5.3		T	2.3I2
A9.I	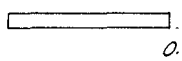 0.5 μm	B	4.79
A9.3		T	2.I3

Key: *B* is the ohmic contact on back of chip only; *S* is the ohmic contact on back and side of chip; *T* is the ohmic contact on back, side, and top to within 13 μm of the anode.

here, included nodal values of potential current densities and electric fields.

VI. DISCUSSION AND CLOSURE

The foregoing sections illustrate that the finite element method is easily applied to the three-dimensional steady-state analysis of Schottky barrier diodes. Particular advantages of this method are ease of dealing with complex shapes and of mesh grading in regions of rapidly varying potential. The mesh grading capability is paramount in Schottky barrier diodes analysis, in which near-singular conditions exist in the anode region. This advantage of the finite element method contrasts strongly with the finite difference method in which mesh grading is considerably more difficult.

The method developed can also be used or adopted for other devices such as Gunn, IMPATT, and other diodes and can also be extended to transistor structures.

The results of the parametric study suggest that the following general conclusions are valid.

The spreading resistance reduces as the anode diameter increases, i.e., as anode surface area moves out from the center.

The ohmic contact configuration greatly affects the spreading resistance; R_{sk} is greatly reduced as the ohmic contact is brought closer towards the anode.

For a prescribed constant anode area the spreading resistance is substantially reduced by distributing the surface area of the anode out from the center.

The rectangular anode shape is optimal.

VII. ACKNOWLEDGMENT

The authors gratefully acknowledge financial support provided by the National Board for Science and Technology, Ireland.

REFERENCES

[1] W. M. Kelly and G. T. Wrixon, "Optimization of Schottky barrier diodes for low noise, low conversion loss operation at near-millimeter wavelengths," in *Infrared and Millimeter Wavelengths*, vol. III, K. J. Button, Ed., New York: Academic Press, 1980.

[2] W. M. Kelly and G T. Wrixon, "Conversion losses in Schottky barrier mixers in the submillimeter region," *IEEE Trans. Microwave Theory Tech* , vol. MTT-27, no. 7, p. 665, July 1979.

[3] G. T. Wrixon and R. F. W Pease, "Schottky barrier diodes fabricated on epitaxial GaAs using electron beam lithography," in *Proc. Inst. Phys. Conf. Series No. 24*, Ch. 2, pp. 55–60, 1975.

[4] J. B. Langley II, "Finite element analysis and electron beam lithographic fabrication of gallium arsenide Schottky barrier diodes with sub-micron features," Ph.D. thesis, National University of Ireland, March 1980.

[5] H. K Gummel, "A self-consistent scheme for one-dimensional steady state transistor calculations," *IEEE Trans. Electron Devices*, vol. ED-11, pp. 455–465, 1964.

[6] J. W. Slotboom, "Computer aided two-dimensional analysis of bipolar transistors," *IEEE Trans. Electron Devices*, vol. ED-20, pp. 869–879, August 1973

[7] J. J. Barnes and R. J. Lomax, "Two-dimensional finite element simulation of semiconductor devices," *Electron. Lett* vol. 10, pp. 341–343, Aug. 1974.

[8] T. Adachi, A. Yoahii, and T. Sado, "Two-dimensional semiconductor analysis using finite element analysis," *IEEE Trans. Electron Devices*, vol. ED-26, pp. 1026–1031, July 1979.

[9] F. B Hildebrand, *Methods of Applied Mathematics*. New York: Prentice–Hall, 1952.

[10] B. Irons and S. Ahmad, *Techniques of Finite Elements*. Chichester: Wiley, 1980

[11] O. C. Zienkiewicz, *The Finite Element Method*, 3rd Ed London, McGraw–Hill, 1977.

John S. Campbell served an engineering apprenticeship before attending a mechanical engineering degree course in Strath-Clyde University, Scotland. After being awarded the B.Sc. degree in 1964 he worked in the Central Electricity Generating Board research division in Berkeley Laboratories, England, where he developed computational methods for the solution of problems encountered in large-scale nuclear and conventional power plants. From 1969 to 1972 he carried out research in finite element methods, at University College, Swansea, and was awarded a Ph.D. for this work.

Since 1973 he has held the position of Lecturer in University College Cork, Ireland. His present research interests center on the development and application of finite element methods in civil, mechanical, and electrical engineering.

Dr. Campbell is a Chartered Engineer and a member of the Institution of Mechanical Engineers, London.

Gerard T. Wrixon (M'75) was born in Limerick, Ireland, on May 25, 1940. He received the B.E. degree from the National University of Ireland, Cork, Ireland, the M.Sc. degree from the California Institute of Technology, Pasadena, and the Ph.D. degree from the University of California, Berkeley, all in electrical engineering, in 1961, 1964, and 1969, respectively.

From 1961 to 1963 he was with Fokker, the Royal Netherlands Aircraft Factory, Amsterdam, the Netherlands, as a Research and Development Engineer. From 1964 to 1965 he was an Instructor in the Electrical Engineering Department at Loyola University, Los Angeles, CA. While a graduate student at the University of California, Berkeley, he served as a Research Assistant in the Radio Astronomy Laboratory and Acting Instructor in the Electrical Engineering Department. From 1969 to 1974 he was a Member of the Technical Staff at the Crawford Hill Laboratory, Bell Laboratories, Holmdel, NJ. He is currently Associate Professor of Electrical Engineering Department at University College Cork, Ireland, and Director of the Microelectronics Research Center.

Dr. Wrixon was the recipient of the Microwave Prize at the 1978 European Microwave Conference.

Millimeter-Wave Performance of Shielded Slot-Lines

ABDEL-MONIEM A. EL-SHERBINY, MEMBER, IEEE

Abstract—**The high frequency characteristics of shielded slot-lines are investigated using a modified Wiener–Hopf technique. The analysis includes the case of uniaxially anisotropic substrates when the principal axis is directed normal to the substrate. The obtained solution is especially useful at higher frequencies where other methods tend to be less effective. Numerical results are given for lines on high dielectric constant substrates over the full usable frequency range. It is shown that lines can be used as transmission elements up to a certain limiting frequency beyond which they will radiate. Physical aspects of the propagation in slot-lines are discussed and the effect of the shields on the properties of the guided modes is explained.**

I. Introduction

SLOT-LINES are attracting increasing interest as a transmission element in integrated circuits at higher microwave and millimeter-wave frequencies. Since their introduction by Cohn and others [1], [2], they have been investigated by a number of authors. At lower microwave frequencies, slot-lines were not much used because of the availability of other efficient and easy-to-calculate transmission lines. At higher frequencies, however, as microstrip lines and waveguides become inadequate for some applications and alternatives are searched, the slot-line becomes a promising element in many respects. The waveguide-housed counterparts, unilateral fin-lines, have been successfully used for many millimeter-wave applications. The slot-line as an open structure was felt to be susceptible to excessive radiation at the discontinuities and to cross-coupling. At higher frequencies, shielded slot-lines may be as efficient as fin-lines and are much easier to integrate. One of the important factors interfering with the application of slot-lines is the lack of data on its performance at higher frequencies. Being inherently non-TEM line, it is much more difficult to calculate, compared to microstrip lines or fin-lines. The latter are frequently treated as ridged rectangular waveguides.

The results of [1], [2] are based on waveguide iris impedance concepts and are sufficiently accurate for narrow slot-lines. Various approaches were suggested for the full-wave treatment of these lines and a fair amount of data is now available [2]–[6]. However, the basic features of prop-

Manuscript received August 19, 1981; revised December 4, 1981.

The author is with Spectra Research Systems, 1811 Quail St., Newport Beach, CA 92660.

0018-9480/82/0500-0750$00.75 ©1982 IEEE